Observation of contemporaneous optical radiation from a γ-ray burst

C. Akerlof*, R. Balsano†, S. Barthelmy‡§, J. Bloch†, P. Butterworth‡‖, D. Casperson†, T. Cline‡, S. Fletcher†, F. Frontera¶, G. Gisler†, J. Heise#, J. Hills†, R. Kehoe*, B. Lee*, S. Marshall☆, T. McKay*, R. Miller†, L. Piro**, W. Priedhorsky†, J. Szymanski† & J. Wren†

* *University of Michigan, Ann Arbor, Michigan 48109, USA*
† *Los Alamos National Laboratory, Los Alamos, New Mexico 87545, USA*
‡ *NASA/Goddard Space Flight Center, Greenbelt, Maryland 20771, USA*
§ *Universities Space Research Association, Seabrook, Maryland 20706, USA*
‖ *Raytheon Systems, Lanham, Maryland 20706, USA*
¶ *Università degli Studi di Ferrara, Ferrara, Italy*
# *Space Research Organization, Utrecht, The Netherlands*
☆ *Lawrence Livermore National Laboratory, Livermore, California 94550, USA*
** *Instituto Astrofisica Spaziale, Rome, Italy*

The origin of γ-ray bursts (GRBs) has been enigmatic since their discovery[1]. The situation improved dramatically in 1997, when the rapid availability of precise coordinates[2,3] for the bursts allowed the detection of faint optical and radio afterglows—optical spectra thus obtained have demonstrated conclusively that the bursts occur at cosmological distances. But, despite efforts by several groups[4–7], optical detection has not hitherto been achieved during the brief duration of a burst. Here we report the detection of bright optical emission from GRB990123 while the burst was still in progress. Our observations begin 22 seconds after the onset of the burst and show an increase in brightness by a factor of 14 during the first 25 seconds; the brightness then declines by a factor of 100, at which point (700 seconds after the burst onset) it falls below our detection threshold. The redshift of this burst, $z \approx 1.6$ (refs 8, 9), implies a peak optical luminosity of 5×10^{49} erg s^{-1}. Optical emission from γ-ray bursts has been generally thought to take place at the shock fronts generated by interaction of the primary energy source with the surrounding medium, where the γ-rays might also be produced. The lack of a significant change in the γ-ray light curve when the optical emission develops suggests that the γ-rays are not produced at the shock front, but closer to the site of the original explosion[10].

The Robotic Optical Transient Search Experiment (ROTSE) is a programme optimized to search for optical radiation contemporaneous with the high-energy photons of a γ-ray burst. The basis for such observations is the BATSE detector on board the Compton Gamma-Ray Observatory. Via rapid processing of the telemetry data stream, the GRB Coordinates Network[11] (GCN) can supply estimated coordinates to distant observatories within a few seconds of the burst detection. The typical error of these coordinates is 5°. A successful imaging system must match this field of view to observe the true burst location with reasonable probability.

The detection reported here was performed with ROTSE-I, a two-by-two array of 35 mm camera telephoto lenses (Canon *f*/1.8, 200 mm focal length) coupled to large-format CCD (charge-coupled device) imagers (Thomson 14 μm 2,048 × 2,048 pixels). All four cameras are co-mounted on a single rapid-slewing platform capable of pointing to any part of the sky within 3 seconds. The cameras are angled with respect to each other, so that the composite field of view is 16° × 16°. This entire assembly is bolted to the roof of a communications enclosure that houses the computer control system. A motor-driven flip-away cover shields the detector from precipitation and direct sunlight. Weather sensors provide the vital information to shut down observations when storms appear, augmented by additional logic to protect the instrument in case of power loss or computer failure. The apparatus is installed at Los Alamos National Laboratory in northern New Mexico.

Since March 1998, ROTSE-I has been active for ~75% of the total available nights, with most of the outage due to poor weather. During this period, ROTSE-I has responded to a total of 53 triggers. Of these, 26 are associated with GRBs and 13 are associated with soft γ-ray repeaters (SGRs). The median response time from the burst onset to start of the first exposure is 10 seconds.

During most of the night, ROTSE-I records a sequence of sky patrol images, mapping the entire visible sky with two pairs of exposures which reach a 5σ V magnitude threshold sensitivity (m_v) of 15. These data, approximately 8 gigabytes, are archived each night for later analysis. A GCN-provided trigger message interrupts any sequence in progress and initiates the slew to the estimated GRB location. A series of exposures with graduated times of 5, 75 and 200 seconds is then begun. Early in this sequence, the platform is 'jogged' by ±8° on each axis to obtain coverage of a four times larger field of view.

At 1999 January 23 09:46:56.12 UTC, an energetic burst triggered the BATSE detector. This message reached Los Alamos 4 seconds later and the first exposure began 6 seconds after this. Unfortunately, a software error prevented the data from being written to disk. The first analysable image was taken 22 seconds after the onset of the burst. The γ-ray light curve for GRB990123 was marked by an initial slow rise, so the BATSE trigger was based on relatively limited statistics. Thus the original GCN position estimate was displaced by 8.9° from subsequent localization, but the large ROTSE-I field of view was sufficient to contain the transient image. At 3.8 hours after the burst, the BeppoSAX satellite provided an X-ray localization[12] in which an optical afterglow was discovered by Odewahn *et al.*[13] at Mt Palomar. This BeppoSAX position enabled rapid examination of a small region of the large ROTSE-I field. A bright and rapidly varying transient was found in the ROTSE images at right ascension (RA) 15 h 25 min 30.2 s, declination (dec.) 44° 46′ 0″, in excellent agreement with the afterglow found by Odewahn *et al.* (RA 15 h 25 min 30.53 s, dec. 44° 46′ 0.5″). Multiple absorption lines in the spectrum of the optical afterglow indicate a redshift of $z > 1.6$. Dark-subtracted and flattened ROTSE-I images of the GRB field are shown in Fig. 1. Details of the light curve are shown in Table 1.

By the time of the first exposure, the optical brightness of the transient had risen to $m_v = 11.7$ mag. The flux rose by a factor of 13.7 in the following 25 seconds and then began a rapid, apparently smooth, decline. This decline began precipitously, with a power-law slope of ~−2.5 and gradually slowed to give a slope of ~−1.5. This decline, 10 minutes after the burst, agrees well with the power-law slope found hours later in early afterglow measurements[14]. These observations cover the transition from internal burst emission to external afterglow emission. The composite light curve is shown in Fig. 2.

Table 1 ROTSE-I observations

Exposure start	Exposure duration	Magnitude	Camera
−7,922.08	75	<14.8	C
22.18	5	11.70 ± 0.07	A
47.38	5	8.86 ± 0.02	A
72.67	5	9.97 ± 0.03	A
157.12	5	11.86 ± 0.13	C
281.40	75	13.07 ± 0.04	A
446.67	75	13.81 ± 0.07	A
611.94	75	14.28 ± 0.12	A
2,409.86	200	<15.6	A
5,133.98	800	<16.1	A

Exposure start times are listed in seconds, relative to the nominal BATSE trigger time (1999 January 23.407594 UT). Exposure durations are in seconds. Magnitudes are in the "V equivalent" system described in Fig. 1 legend. Errors include both statistical errors and systematic errors arising from zero-point calibration. They do not include errors due to variations in the unknown spectral slope of the emission. Magnitude limits are 5σ. The final limit results from co-adding the last four 200-s exposures and is quoted at the mean time of those exposures. Camera entries record the camera in which each observation was made.

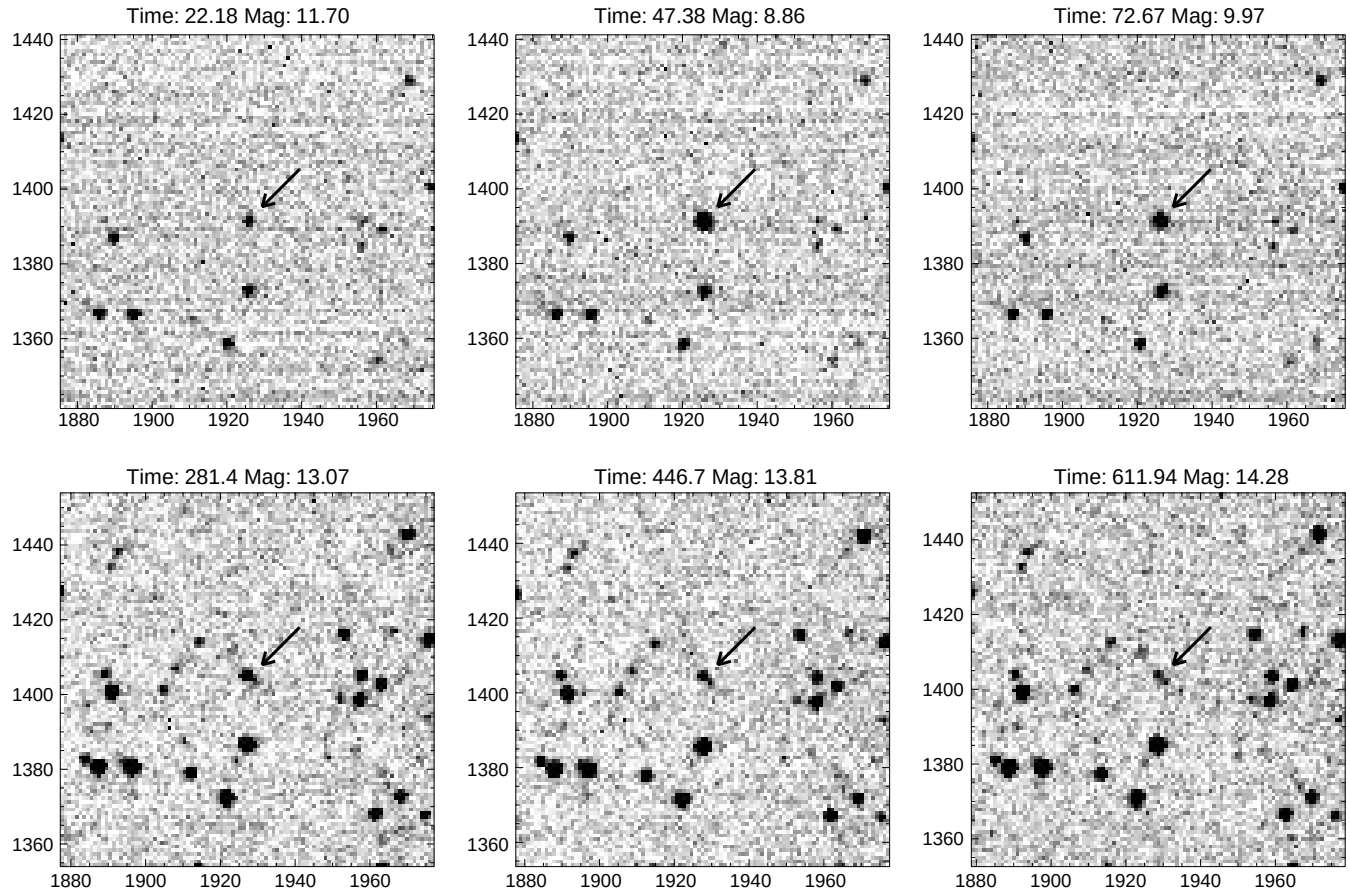

Figure 1 Time series images of the optical burst. Each image is 24′ on a side, and represents 6×10^{-4} of the ROTSE-I field of view. The horizontal and vertical axes are the CCD pixel coordinates. The sensitivity variations are due to exposure time; the top three images are 5-s exposures, the bottom three are 75-s exposures. The optical transient (OT) is clearly detected in all images, and is indicated by the arrow. South is up, east is left. Thermal effects are removed from the images by subtracting an average dark exposure. Flat field images are generated by median averaging about 100 sky patrol (see text) images. Object catalogues are extracted from the images using SExtractor[18]. Astrometric and photometric calibrations are determined by comparison with the ~1,000 Tycho[19] stars available in each image. Residuals for stars of magnitude 8.5–9.5 are <1.2″. These images are obtained with unfiltered CCDs. The optics and CCD quantum efficiency limit our sensitivity to a wavelength range between 400 and 1,100 nm. Because this wide band is non-standard, we estimate a ''V equivalent'' magnitude by the following calibration scheme. For each Tycho star, a ''predicted ROTSE magnitude'' is compared to the 2.5 pixel aperture fluxes measured for these objects to obtain a global zero point for each ROTSE-I image. For the Tycho stars, the agreement between our predicted magnitude and the measured magnitude is ±0.15. These errors are dominated by colour variation. The zero points are determined to ±0.02. With large pixels, we must understand the effects of crowding. (This is especially true as we follow the transient to ever fainter magnitudes.) To check the effect of such crowding, we have compared the burst location to the locations of known objects from the USNO A V2.0 catalogue[20]. The nearest object, 34″ away, is a star with R-band magnitude $R = 19.2$. More important is an $R = 14.4$ star, 42″ away. This object affects the measured magnitude of the OT only in our final detection. It can be seen in the final image to the lower right of the OT. A correction of +0.15 is applied to compensate for its presence. Magnitudes for the OT associated with GRB990123, measured as described, are listed in Table 1. Further information about the ROTSE-I observations is available at http://www.umich.edu/~rotse.

A number of arguments establish the association of our optical transient with the burst and the afterglow seen later. First, the statistical significance of the transient image exceeds 160σ at the peak. Second, the temporal correlation of the light curve with the GRB flux and the spatial correlations to the X-ray and afterglow positions argue strongly for a common origin. Third, the most recent previous sky patrol image was taken 130 minutes before the burst and no object is visible brighter than $m_v = 14.8$ mag. This is the most stringent limit on an optical precursor obtained to date. Searches further back in time (55 images dating to 28 September 1998) also find no signal. Finally, the 'axis jogging' protocol places the transient at different pixel locations within an image and even in different cameras throughout the exposure series, eliminating the possibility of a CCD defect or internal 'ghost' masquerading as a signal.

The fluence of GRB990123 was exceptionally high (99.6 percentile of BATSE triggers; M. Briggs, personal communication), implying that such bright optical transients may be rare. Models of early optical emission suggest that optical intensity scales with γ-ray fluence[15–17]. If this is the case, ROTSE-I and similar instruments are sensitive to 50% of all GRBs. This translates to ~12 optically detected events per year. Our continuing analysis of less well-localized GRB data may therefore reveal similar transients. To date, this process has been hampered by the necessity of identifying and discarding typically 100,000 objects within the large field of view and optimizing a search strategy in the face of an unknown early time structure. The results we report here at least partially resolve the latter problem while increasing the incentive to complete a difficult analysis task. The ROTSE project is in the process of completing two 0.45-m telescopes capable of reaching 4 magnitudes deeper than ROTSE-I for the same duration exposures. If γ-ray emission in bursts is beamed but the optical emission is more isotropic, there may be many optical transients unassociated with detectable GRBs. These instruments will conduct sensitive searches

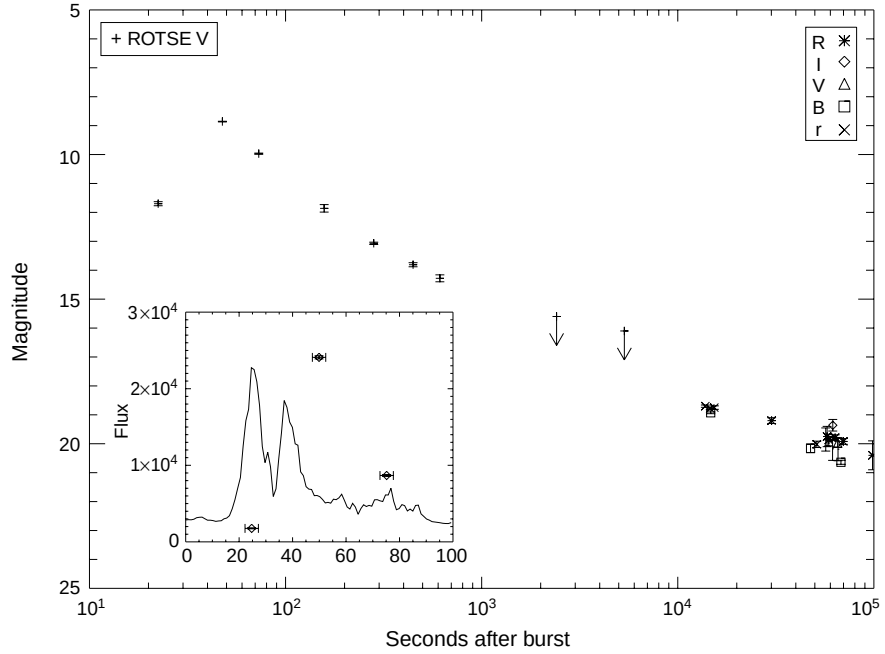

Figure 2 A combined optical light curve. Afterglow data points are drawn from the GCN archive[21–33]. The early decay of the ROTSE-I light curve is not well fitted by a single power law. The final ROTSE limit is obtained by co-adding the final four 200-s images. The inset shows the first three ROTSE optical fluxes compared to the BATSE γ-ray light curve in the 100–300 keV energy band. The ROTSE-1 fluxes are in arbitrary units. Horizontal error bars indicate periods of active observation. We note that there is no information about the optical light curve outside these intervals. Vertical error bars represent flux uncertainties. Further information about GCN is available at http://gcn.gsfc.nasa.gov/gcn

for such events. We expect that ROTSE will be important in the exploration to come. □

Received 5 February; accepted 19 February 1999.

1. Klebesadel, R. W., Strong, I. B. & Olson, R. A. Observations of gamma-ray bursts of cosmic origin. *Astrophys. J.* **182,** L85–L88 (1973).
2. Piro, L. *et al.* The first X-ray localization of a γ-ray burst by BeppoSAX and its fast spectral evolution. *Astron. Astrophys.* **329,** 906–910 (1998).
3. Costa, E. *et al.* Discovery of an X-ray afterglow associated with the γ-ray burst of 28 February 1997. *Nature* **387,** 783–785 (1997).
4. Krimm, H. A., Vanderspek, R. K. & Ricker, G. R. Searches for optical counterparts of BATSE gamma-ray bursts with the Explosive Transient Camera. *Astron. Astrophys. Suppl.* **120,** 251–254 (1996).
5. Hudec, R. & Soldán, J. Ground-based optical CCD experiments for GRB and optical transient detection. *Astrophys. Space Sci.* **231,** 311–314 (1995).
6. Lee, B. *et al.* Results from Gamma-Ray Optical Counterpart Search Experiment: a real time search for gamma-ray burst optical counterparts. *Astrophys. J.* **482,** L125–L129 (1997).
7. Park, H. S. *et al.* New constraints on simultaneous optical emission from gamma-ray bursts measured by the Livermore Optical Transient Imaging System experiment. *Astrophys. J.* **490,** L21–L24 (1997).
8. Kelson, D. D., Illingworth, G. D., Franx, M., Magee, D. & van Dokkum, P. G. *IAU Circ.* No. 7096 (1999).
9. Hjorth, J. *et al. GCN Circ.* No. 219 (1999).
10. Fenimore, E. E., Ramirez-Ruiz, E., Wu, B. GRB990123: Evidence that the γ-rays come from a central engine. Preprint astro-ph9902007 at ⟨http://xxx.lanl.gov⟩ (1999).
11. Barthelmy, S. *et al.* in *Gamma-Ray Bursts: 4th Huntsville Symp.* (eds Meegan, C. A, Koskut, T. M. & Preece, R. D.) 99–103 (AIP Conf. Proc. 428, Am. Inst. Phys., College Park, 1997).
12. Piro, L. *et al. GCN Circ.* No. 199 (1999).
13. Odewahn, S. C. *et al. GCN Circ.* No. 201 (1999).
14. Bloom, J. S. *et al. GCN Circ.* No. 208 (1999).
15. Katz, J. I. Low-frequency spectra of gamma-ray bursts. *Astrophys. J.* **432,** L107–L109 (1994).
16. Mészáros, P. & Rees, M. J. Optical and long-wavelength afterglow from gamma-ray bursts. *Astrophys. J.* **476,** 232–237 (1997).
17. Sari, R. & Piran, T. The early afterglow. Preprint astro-ph/9901105 at ⟨http://xxx.lanl.gov⟩ (1999).
18. Bertin, E. & Arnouts, S. SExtractor: Software for source extraction. *Astron. Astrophys. Suppl.* **117,** 393–404 (1996).
19. Høg, E. *et al.* The Tycho reference catalogue. *Astron. Astrophys.* **335,** L65–L68 (1998).
20. Monet, D. *et al. A Catalog of Astrometric Standards* (US Naval Observatory, Washington DC, 1998).
21. Zhu, J. & Zhang, H. T. *GCN Circ.* No. 204 (1999).
22. Bloom, J. S. *et al. GCN Circ.* No. 206 (1999).
23. Gal, R. R. *et al. GCN Circ.* No. 207 (1999).
24. Sokolov, V. *et al. GCN Circ.* No. 209 (1999).
25. Ofek, E. & Leibowitz, E. M. *GCN Circ.* No. 210 (1999).
26. Garnavich, P., Jha, S., Stanek, K. & Garcia, M. *GCN Circ.* No. 215 (1999).
27. Zhu, J. *et al. GCN Circ.* No. 217 (1999).
28. Bloom, J. S. *et al. GCN Circ.* No. 218 (1999).
29. Maury, A., Boer, M. & Chaty, S. *GCN Circ.* No. 220 (1999).
30. Zhu, J. *et al. GCN Circ.* No. 226 (1999).
31. Sagar, R., Pandey, A. K., Yadav, R. K. R., Nilakshi & Mohan, V. *GCN Circ.* No. 227 (1999).
32. Masetti, N. *et al. GCN Circ.* No. 233 (1999).
33. Bloom, J. S. *et al. GCN Circ.* No. 240 (1999).

Acknowledgements. the ROTSE Collaboration thanks J. Fishman and the BATSE team for providing the data that enable the GCN localizations which made this experiment possible; and we thank the BeppoSAX team for rapid distribution of coordinates. This work was supported by NASA and the US DOE. The Los Alamos National Laboratory is operated by the University of California for the US Department of Energy (DOE). The work was performed in part under the auspices of the US DOE by Lawrence Livermore National Laboratory. BeppoSAX is a programme of the Italian Space Agency (ASI) with participation of the Dutch Space Agency (NIVR).

Correspondence and requests for materials should be addressed to C.A. (e-mail: akerlof@mich.physics.lsa.umich.edu).

A simple explanation of light emission in sonoluminescence

Sascha Hilgenfeldt*, Siegfried Grossmann† & Detlef Lohse‡

** Division of Engineering and Applied Sciences, Harvard University, 29 Oxford Street, Cambridge, Massachusetts 02138, USA*
† Fachbereich Physik der Universität Marburg, Renthof 6, D-35032 Marburg, Germany
‡ Department of Applied Physics and J. M. Burgers Centre for Fluid Dynamics, University of Twente, PO Box 217, NL-7500 AE Enschede, The Netherlands

Ultrasonically driven gas bubbles in liquids can emit intense bursts of light when they collapse[1]. The physical mechanism for single-bubble sonoluminescence has been much debated[2,3]. The conditions required for, and generated by, bubble collapse can be deduced within the framework of a hydrodynamic (Rayleigh–Plesset[4]) analysis of bubble dynamics and stability[5,6], and by considering the dissociation and outward diffusion of gases under the extreme conditions induced by collapse[7,8]. We show here that by extending this hydrodynamic/chemical picture in a simple way, the light emission can be explained too. The additional elements that we add are a model for the volume dependence of the bubble's temperature[9,10] and allowance for the small emissivity of a weakly ionized gas[11]. Despite its simplicity, our approach can account quantitatively for the observed parameter dependences of